forests

MDPI

Article

Sediment CO_2 Flux from a Mangrove in Southern China: Is It Controlled by Spatiotemporal, Biotic or Physical Factors?

Siqi Nie [1,2,†], Xiaoguang Ouyang [1,2,*,†], Wenqing Wang [3], Zhenchang Zhu [2], Fen Guo [2], Zhifeng Yang [1,2] and Shing Yip Lee [4]

1 Research Centre of Ecology & Environment for Coastal Area and Deep Sea, Southern Marine Science and Engineering Guangdong Laboratory (Guangzhou), Guangzhou 511458, China
2 Guangdong Provincial Key Laboratory of Water Quality Improvement and Ecological Restoration for Watersheds, School of Ecology, Environment and Resources, Guangdong University of Technology, Guangzhou 510006, China
3 Key Laboratory of the Ministry of Education for Coastal and Wetland Ecosystems, College of the Environment and Ecology, Xiamen University, Xiamen 361102, China
4 Simon F. S. Li Marine Science Laboratory, School of Life Sciences, The Chinese University of Hong Kong, Shatin, Hong Kong, China
* Correspondence: x.ouyang@gmlab.ac.cn
† These authors contribute equally to this work.

Abstract: Carbon gas flux is important for studies on carbon dynamics in mangroves, but the controlling factors have not always been sufficiently understood. In this study, it is suggested that sediment carbon dioxide (CO_2) fluxes in a natural mangrove in Southern China are controlled by tidal positions, seasons, species, the densities of crab burrows and pneumatophores, light conditions and sediment temperature. All these factors account for 51.47% variation in CO_2 flux from the sediment–air interface. CO_2 flux generally decreased along the tidal position from landward to seaward, and was higher in the dry season than in the wet season. CO_2 flux was highest in *Avicennia* marina (grey mangrove) in comparison with *Aegiceras corniculatum* (river mangrove) and *Kandelia obovata*. Pneumatophores and crab burrows promoted sediment CO_2 flux in the mangrove at a rate of 18.29 and 15.52 mmol m^{-2} d^{-1}. Dark flux was higher than light flux. Sediment temperature has a negative influence on CO_2 flux. Pneumatophores explain the most variation (13.9%) in CO_2 flux among the above factors. Our study suggests that the photosynthesis activity of microphytobenthos is an important factor driving the change of CO_2 emissions in this natural mangrove. This is of great significance for the study and for the full exploitation of the carbon sink potential of mangroves.

Keywords: mangrove; CO_2 flux; pneumatophore; crab burrow; tidal position; light; species; season

check for updates

Citation: Nie, S.; Ouyang, X.; Wang, W.; Zhu, Z.; Guo, F.; Yang, Z.; Lee, S.Y. Sediment CO_2 Flux from a Mangrove in Southern China: Is It Controlled by Spatiotemporal, Biotic or Physical Factors? *Forests* **2023**, *14*, 782. https://doi.org/10.3390/f14040782

Academic Editor: Ilona Mészáros

Received: 4 March 2023
Revised: 27 March 2023
Accepted: 30 March 2023
Published: 11 April 2023

1. Introduction

Mangroves have been credited with a highly productive ecosystem and high sediment carbon (C) accumulation capacity [1]. In particular, they are among the most carbon-rich forests in the tropics [2]. They are increasingly regarded as C rich ecosystems that warrant restoration and preservation [3], considered to be able to assume a role in regulating climate, sequestering and preserving noticeable amounts of C to help counteract anthropogenic carbon dioxide (CO_2) emissions [4,5]. During 2003 to 2010, total wetland C stocks increased by 22% due to mangrove encroachment into salt marshes along the eastern coast of Florida, USA [6]. Mangrove C stocks can also change due to land use change, and natural growth and regeneration [7]. Accordingly, studies in terms of mangrove C dynamics have been listed as one of the focuses in the discussion of mangroves over the past five decades [8].

Among the research branches of mangrove C dynamics, C gas flux attracts attention in mangrove research communities, and specific studies contribute to the understanding of net ecosystem productivity (NEP) and other ecosystem processes. CO_2 flux from sediments

is a noticeable fraction of C loss. Specifically, the quantification of CO_2 flux is significant, since 94%–98% of sediment organic carbon (OC) losses in mangroves result from microbial respiration, i.e., CO_2 flux [9]. Measurements of sediment CO_2 flux in mangroves have a great potential to serve as an indicator of ecosystem processes, including sediment metabolic activity, persistence and decay of plant residue (such as root and rhizosphere material) in sediments, and conversion of sediment OC to CO_2 [10,11].

The release of CO_2 via the sediment–air interface includes CO_2 flux from litter decomposition, roots and heterotrophic respiration [12–14], and tends to be measured by the closed dynamic chamber (CDC) technique. The net primary productivity (NPP) and heterotrophic respiration in sediments permit the estimation of NEP. Similar extrapolation of C budgets in global mangrove ecosystems used the heterotrophic CO_2 flux as a proxy for C mineralization in sediments [15]. The heterotrophic respiration in sediments follows a sequence on the ground of the availability of electron acceptors, which is associated with vertical changes in redox chemistry and population abundance of the different metabolic types of bacteria [16]. The main pathways of sediment heterotrophic respiration include aerobic respiration, sulphate reduction, manganese reduction, iron reduction and denitrification. Because sediments have microzones where some of these metabolic processes coexist, what all of these processes have in common is the production of CO_2, as it can be measured at the sediment surface in closed chambers to give an estimate of the total heterotrophic respiration of C.

CO_2 flux from the sediment–air interface in mangroves has been found to vary with sediment properties, tidal positions [17], seasons and species [18], and be modulated by crab burrows and pneumatophores [19]. However, past studies tended to examine the variation in CO_2 flux with only some of the aforementioned factors. In addition, [19] investigated the increase of CO_2 release due to the occurrence of pneumatophores, but did not establish the relationship between CO_2 flux and the densities of pneumatophores. However, this kind of relationship may be attributed to the fact that pneumatophores provide large amounts of oxygen for sediment microbial activities and increase aerobic respiration, thus affecting CO_2 flux [20].

Mangroves are primarily distributed in tropical and subtropical coastal regions. In China, mangroves occur in the southern region where the climate is subtropical. In this study, CO_2 flux measurement was conducted in a natural mangrove in Southern China. We aimed to examine the relationship between CO_2 flux and a variety of variables, including seasons, tidal positions, species, sediment temperature, crab burrow and pneumatophore densities, and to identify the main factors resulting in the variation of sediment CO_2 flux. The result of our study is expected to shed light on the studies of mangrove C flux.

2. Materials and Methods

2.1. Sampling Site

This study was conducted in Zhangjiangkou National Mangrove Nature Reserve (23°53′45″–23°56′00″ N, 117°24′07″–117°24′30″ E) in Yunxiao, Fujian Province, China (Figure 1). The sampling site is located in the mid-to-upper tidal position of the Zhangjiang estuary, which is semi-enclosed and opens into the Taiwan Strait. The estuary occupies ~2360 ha and is forested by 117.9 ha of mangroves. Mangroves in the estuary are dominated by *Avicennia marina* (*grey mangrove*), *Kandelia obovata* and *Aegiceras corniculatum* (*river mangrove*). Seven of 32 National Nature Reserves, established to protect native animal or plant species over China's coast, have been markedly invaded by *Spartina alterniflora*, with the total area accounting for about one-third of the total invasion area in mainland China. Given the rapid expansion of *S. alterniflora* since its introduction and the serious ecological effects, effective response decisions are urgently needed [21]. The invasion of cordgrass *Spartina alterniflora* has resulted in rapid encroachment of the intertidal mudflat seaward to the mangroves, effectively suppressing mangrove expansion into the accreting coast [22]. Table 1 shows the mangrove and saltmarsh species in the studied area. The average annual rainfall was 1583.1 mm, and the average annual temperature was 22.4 °C.

The detailed monthly temperature and rainfall are shown in Table 2. The average water salinity was 19%.

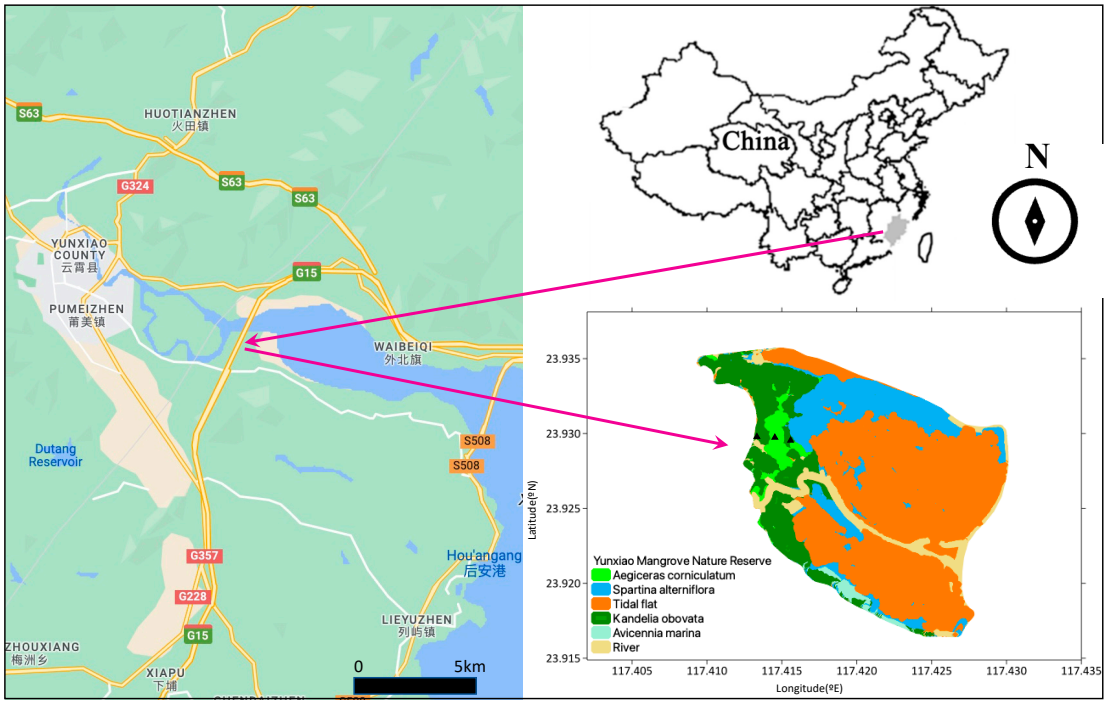

Figure 1. CO_2 flux sampling site in Yunxiao, Fujian Province, China. The triangles in the lower right panel show the sampling points.

Table 1. A list of mangrove and saltmarsh plant species in the studied area.

Scientific Name	Synonym Name	Native/Non-Native
Avicennia marina	grey mangrove	Native
Aegiceras corniculatum	river mangrove	Native
Kandelia obovata	NA	Native
Spartina alterniflora	cordgrass	non-native

Table 2. Monthly temperature and precipitation in 2022 in the studied area.

Climate	January	February	March	April	May	June	July	August	September	October	November	December
Highest temperature (°C)	19	18	24	27	27	31	34	33	34	30	26	20
Lowest temperature (°C)	12	11	15	18	20	24	26	26	24	21	19	12
Precipitation (mm)	8.6	19	2.5	28.9	149.9	302.9	81.7	470.8	7.4	128.1	145.6	4.9

2.2. Sampling Scheme

A four-factorial sampling design (season × tidal position × species × light condition) was considered in this study. While these factors have been considered important in regulating CO_2 fluxes [17,18], they have seldom been examined together. Light conditions were defined as dark or light. The sampling campaigns were conducted in April (wet season) and November (dry season). CO_2 fluxes were measured across a tidal gradient from seaward, middle to landward sites. At each location, sampling was performed in all the dominant species, i.e., *Avicennia marina*, *Kandelia obovata* and *Aegiceras corniculatum*, under both dark and light conditions. Five replicates (plots) were selected randomly. The plots are ~2 m away from each other, and the sampling area at each position is 10 m^2.

2.3. Sampling Methods

In order to standardize the measurements, CO_2 efflux across the sediment–air interface was measured between 9:00 am and 1:00 pm in the mangrove on consecutive days during the sampling campaign. Dark and light CO_2 fluxes were measured using transparent polycarbonate chambers and chambers covered by aluminum foil, respectively. The chambers (diameter 35.5 cm, volume 5.7 L) were pushed 0.5 cm into the sediment 30 min before CO_2 measurement, to allow the set-up to equilibrate while preventing undue difference (e.g., temperature) in conditions between the two chambers. Each chamber has an air pump, and two sampling ports on opposite sides of the chamber through which a stream of air flow was maintained by the air pump at a flow rate of 200 mL min^{-1} to minimize gas build-up in the chamber. Pressure equilibrium between air in the chamber and the surrounding air was maintained by a relief vent in accordance with [23]. CO_2 efflux was measured by an infrared gas analyzer SBA-5 (PP System Inc., Amesbury, MA, USA) up to a 20-min period, until a stable rate lasting for at least 2.5 min was obtained. The short incubation period was selected to avoid excessive environmental microclimatic changes (e.g., water content, sediment temperature and CO_2 concentration gradients), which may influence gas diffusivity [24,25]. Zero calibration was conducted using a soda lime canister after each measurement to ensure accuracy. Sediment CO_2 effluxes were calculated by the following equation:

$$F = \frac{\Delta p\mathrm{CO_2}}{\Delta t}\frac{V}{RTS}$$

where F is the sediment CO_2 efflux (μmol m^{-2} s^{-1}) and was transformed to mmol m^{-2} d^{-1}, divided by a coefficient of 86.4; $\Delta pCO_2/\Delta t$ is the variation in pCO_2 with the measurement time t (ppm s^{-1}); V is the volume of the measurement system (m^3); R is the ideal gas constant of 8.2058×10^{-5} atm m^3 K^{-1} mol^{-1}; T is the air temperature (K); and S is the surface sediment area covered by the chamber (m^2).

During each gas flux measurement, the sediment's physical and hydrological parameters were recorded. Air and sediment temperature as well as humidity were recorded after measurement by sensors. The water level was measured by a line tape after digging a hole in the sampling plot. The number of crab burrows and pneumatophores were counted in each sampling plot. The canopy height of each mangrove species at the study site was extracted from the site map of the canopy height, generated from UAV-borne LiDAR data [26].

2.4. Statistical and Data Analysis

Multiple regression analysis was undertaken to explore the relationship between CO_2 flux and all the factors, including seasons, tidal positions, species, light conditions, sediment temperature and humidity, water level, and the densities of crab burrows and pneumatophores. The assumption of homogeneity was verified by plotting the results of linear regression (similar to the homogeneity test in linear regression). The assumption of normality was tested by the Shapiro–Wilk normality test. Influential values were removed from the data set according to the Cook distance. Stepwise regression analysis was conducted with seasons, tidal positions, species and light conditions input as dummy variables, with one level of each dummy variable setting as the reference. The same multiple regression model was run for both dark and light fluxes to investigate the difference in regression coefficients. Principal component analysis (PCA) was performed to examine the variability of all variables, including CO_2 flux, in the studied site.

Because seasons, tidal positions, species and light conditions are significant in the regression model, the four-way analysis of variance (ANOVA), the random effect model was used to further analyze the variation in CO_2 flux among these factors. The plot is set as a random effect, as there may be variation in CO_2 flux at each plot arising from differences in the sediment's micro-environment, e.g., moisture, shading, the densities of crab burrows and pneumatophores. Data were checked for the possibility of an interaction between the random blocking factor and the main effects by Tukey's test for additivity, and then checked

for sphericity (homogeneity of variances from all pairs of treatment levels) by Mauchly's test. Tukey's HSD test was conducted to examine the difference where there is a significant treatment effect (the number of groups > 3). Paired-sample t test was conducted to compare dark and light CO_2 efflux recorded from the paired chambers, and to compare CO_2 flux in wet and dry seasons from the same location.

The variation of CO_2 effluxes with species, light conditions and species over the mangroves in the nature reserve was mapped by combining the species distribution of the mangroves [26]. A map of average CO_2 efflux at the study site was also generated by averaging CO_2 effluxes by combining seasons and light conditions.

R programming language was used to perform data analysis [27]. The R packages 'asbio' [28], 'car' [29] and 'relaimpo' [30] were employed to perform the Tukey's test for additivity, to check for sphericity and to examine the relative importance of independent variables, respectively. Data are presented as mean ± 1 standard error (SE).

3. Results

3.1. Relationship between CO_2 Flux and Influential Factors

Multiple regression analysis reflects a very significant relationship between sediment CO_2 flux and sediment temperature, crab burrows and pneumatophore densities, seasons, tidal positions and light conditions ($p < 0.001$, Table 3). The combination of the above factors explains the 51.5% variation in sediment CO_2 flux ($R^2 = 0.515$). Amongst these factors, the pneumatophore densities represent most of the variation in CO_2 flux (13.85%), followed by species (12.72%) and light conditions (7.57%), while the variances explained by other factors are all below 5% (Figure 2). PCA analysis showed that the first two components explained 40.1% of the variance in all the variables in the studied mangrove forest. CO_2 flux showed a close positive correlation with pneumatophore densities but negative correlations with light conditions, which is consistent with the results of multiple regression analysis (Figure 3).

Table 3. Relationship between all CO_2 fluxes and independent variables.

CO_2 Fluxes ≈ Sediment Temperature + Burrow + Pneumatophore + Season + Species + Tidal Position + Light Conditions				
	Estimate	**SE**	**t Value**	**Significance**
(Intercept)	19.95	3.66	5.46	***
Sediment temperature	−0.57	0.14	−3.99	***
Burrow	0.39	0.15	2.66	**
Pneumatophore	0.13	0.08	1.57	>0.05
Seasondry	3.27	0.70	4.69	***
Positionmid	−1.24	0.82	−1.52	>0.05
Positionseaward	−3.64	0.82	−4.46	***
SpeciesAM	2.01	1.12	1.79	
SpeciesKO	−0.20	0.91	−0.22	>0.05
LightLight	−6.37	0.62	−10.20	***

Significance codes: 0 '***' 0.001 '**'; AM denotes Avicennia marina. KO denotes Kandelia obovata. $R^2 = 0.515$, $p < 0.001$.

When dark and light fluxes were analyzed separately, a very significant relationship was found between dark flux and species, tidal positions as well as the densities of pneumatophores ($p < 0.001$, Table 4). Likewise, there was a very significant relationship between light flux and sediment temperature, the densities of crab burrows and pneumatophores, seasons as well as tidal positions ($p < 0.001$, Table 5). The above models extrapolate 48.6% and 48.7% of the variance in dark and light flux, respectively ($R^2 = 0.486$ and 0.487).

3.2. Variation in CO_2 Flux with Seasons, Tidal Positions, Species and Light Conditions

Table 6 shows that there were very significant differences in sediment CO_2 flux among different treatments of species, tidal positions, seasons and light conditions, and also the interactions of species × tidal position, species × season (ANOVA, $p < 0.001$), and species

× light condition (ANOVA, $p < 0.01$). In addition, there was a significant interaction effect of tidal position × light condition on the variation in CO_2 flux (ANOVA, $p < 0.05$).

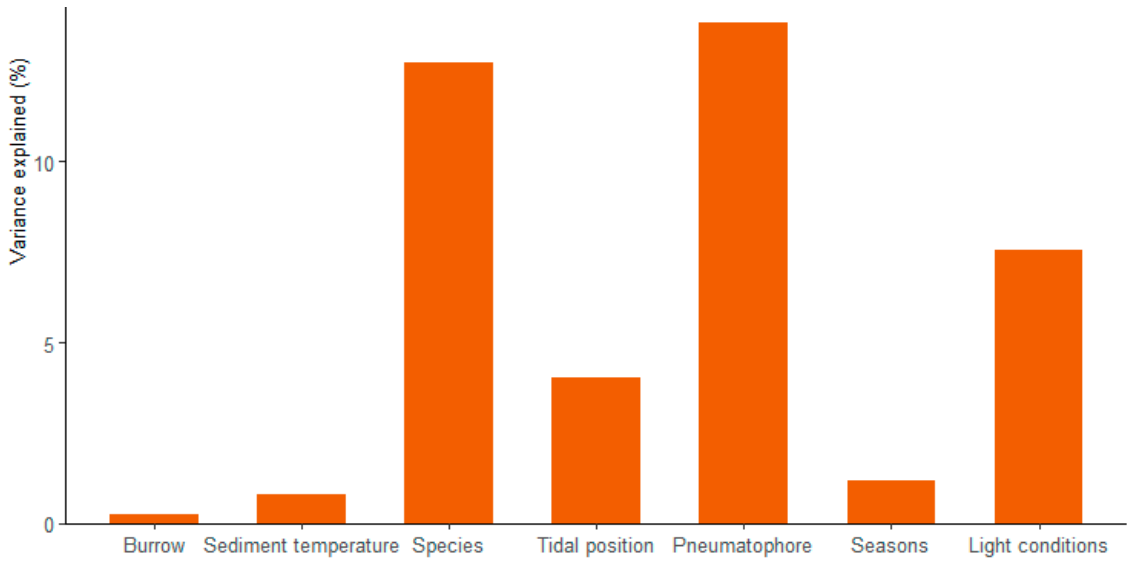

Figure 2. The variance of CO_2 flux explained by individual factors.

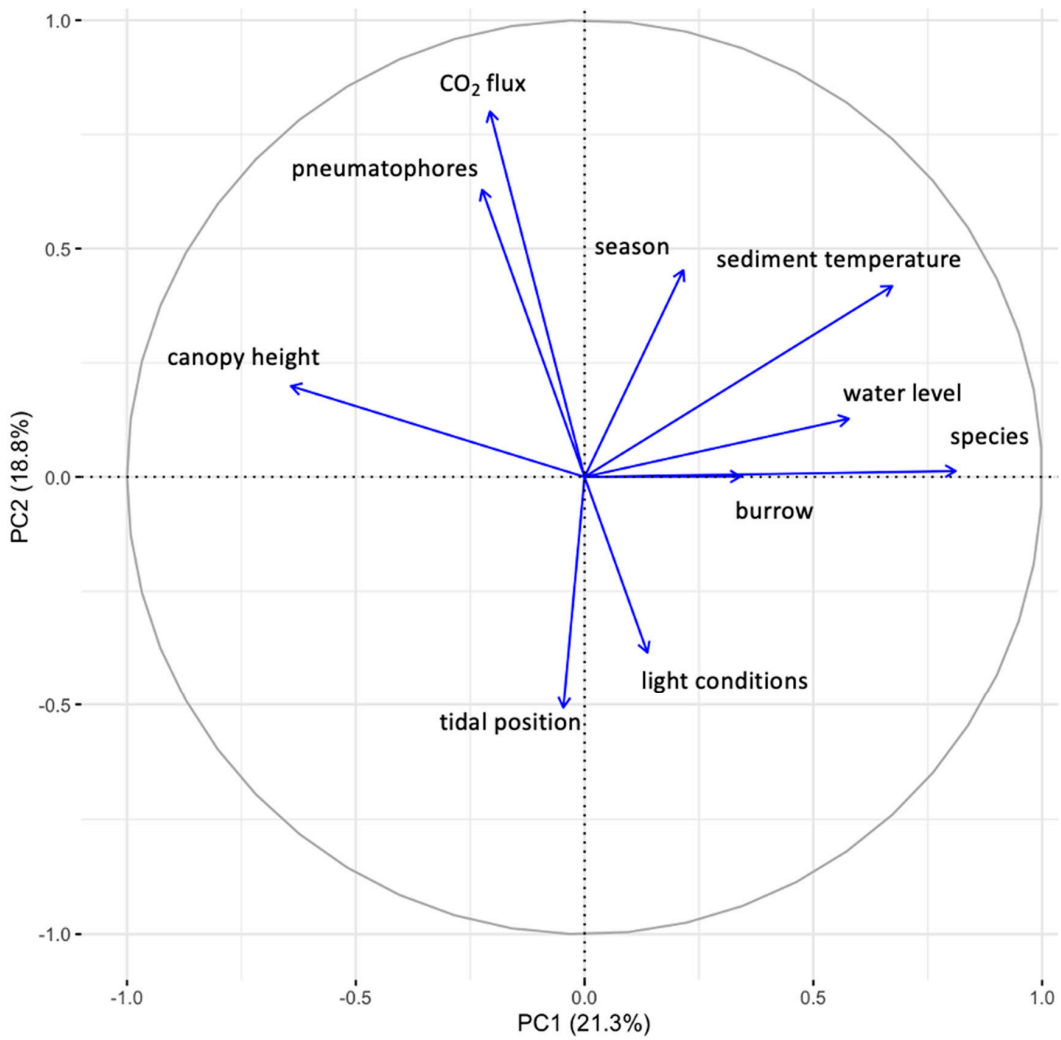

Figure 3. PCA analysis of CO_2 flux and other variables in the studies mangrove.

Table 4. Relationship between dark CO_2 flux and independent variables.

Dark Fluxes ≈ Pdark + Tidal Position + Species				
	Estimate	**SE**	**t Value**	**Significance**
(Intercept)	20.99	1.25	16.86	***
Pdark	0.47	0.14	3.38	**
Positionmid	1.13	1.38	0.82	>0.05
Positionseaward	−2.61	1.37	−1.90	
SpeciesAM	2.85	2.02	1.41	>0.05
SpeciesKO	−2.79	1.37	−2.03	*

Significance codes: 0 '***' 0.001 '**' 0.01 '*'; Pdark: pneumatophores under dark conditions. R^2 = 0.486, $p < 0.001$.

Table 5. Relationship between light CO_2 flux and independent variables.

Light Fluxes ~ Sediment Temperature + BLight + PLight + Tidal Position + Season				
	Estimate	**SE**	**t Value**	**Significance**
(Intercept)	23.72	4.81	4.93	***
Sediment temperature	−1.02	0.20	−5.13	***
BLight	0.57	0.20	2.85	**
PLight	0.36	0.09	4.06	***
Positionmid	−2.37	1.38	−1.72	
Positionseaward	−5.70	1.33	−4.28	***
Seasondry	5.77	1.10	5.24	***

Significance codes: 0 '***' 0.001 '**'; BLight: burrows under light conditions, PLight: pneumatophores under light conditions. R^2 = 0.487, $p < 0.001$.

Table 6. Four-way ANOVA of CO_2 flux variation.

Source of CO_2 Flux Variation	df	Sum Sq	F Value	Significance
Model: CO_2 Flux ≈ Plot + Species × Tidal Position × Season × Light Condition				
Plot (replicate)	4	8939	1.75	>0.05
Species	2	71,774	28.12	***
Tidal position	2	31,033	12.16	***
Season	1	26,564	20.82	***
Light condition	1	84,652	66.33	***
Species: Tidal position	4	29,826	5.84	***
Species: Season	2	19,255	7.54	***
Tidal position: Season	2	2749	1.08	>0.05
Species: Light condition	2	16,865	6.61	**
Tidal position: Light condition	2	9229	3.62	*
Season: Light condition	1	4459	3.49	>0.05
Species: Tidal position: Season	4	8573	1.68	>0.05
Species: Tidal position: Light condition	4	3516	0.69	>0.05
Species: Season: Light condition	2	534	0.21	>0.05
Tidal position: Season: Light condition	2	4139	1.62	>0.05
Species: Tidal position: Season: Light condition	4	3490	0.68	>0.05
Residuals	140	17,866,153		

Significance codes: 0 '***' 0.001 '**' 0.01 '*'; df denotes degree of freedom. Sq denotes square.

Furthermore, CO_2 flux at the seaward sites was significantly lower than at the landward and middle sites (Tukey's HSD test, $p < 0.001$, Figure 4). Similarly, sediment CO_2 flux from *Avicennia marina* was significantly higher than that from both *Aegiceras corniculatum* and *Kandelia obovata* (Tukey's HSD test, $p < 0.001$). Dark flux was significantly higher than light flux (paired sample t-test, $p < 0.001$), while CO_2 flux in the wet season was significantly lower than that in the dry season (paired sample t-test, $p < 0.01$). Further, CO_2 flux varied under different scenarios among the combinations of 2 factors, including species × tidal position, species × light conditions, species × seasons, and tidal positions × seasons. CO_2 flux was significantly higher in *Avicennia marina* at the landward and mid locations

(scenario 1, Tukey's HSD test, $p < 0.001$), in *A. marina* under dark conditions (scenario 2, Tukey's HSD test, $p < 0.01$), in *Avicennia marina* in dry seasons (scenario 3, Tukey's HSD test, $p < 0.001$) and at mid locations under dark conditions (scenario 4, Tukey's HSD test, $p < 0.05$), in contrast to others. The spatial variation of CO_2 fluxes over the mangroves in the Zhangjiangkou National Mangrove Nature Reserve was mapped by considering the variation of CO_2 fluxes with seasons, light conditions and species (Figure 5). The average annual dark and light CO_2 fluxes in the studied site reached 21.5 ± 1.9 mol m^{-2} yr^{-1} and 5.6 ± 1.9 mol m^{-2} yr^{-1}, respectively. Combining the dark and light flux, the average annual CO_2 flux reached 13.6 ± 1.5 mol m^{-2} yr^{-1} (Figure 6).

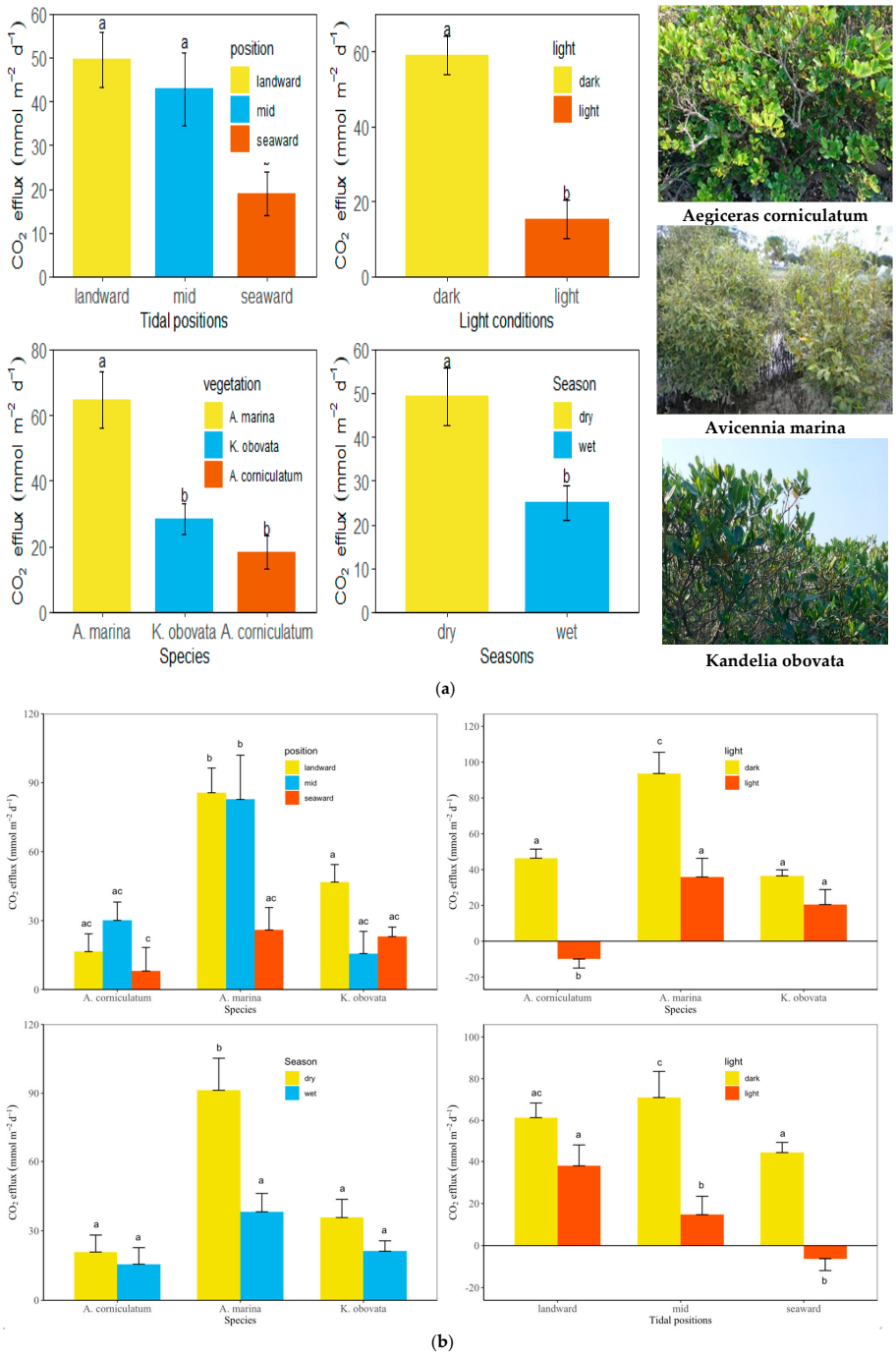

Figure 4. Differences of CO_2 flux among tidal positions, species, light conditions and seasons (**a**) and combinations of 2 factors (**b**). Error bars labelled with different letters suggest there is a significant difference in values.

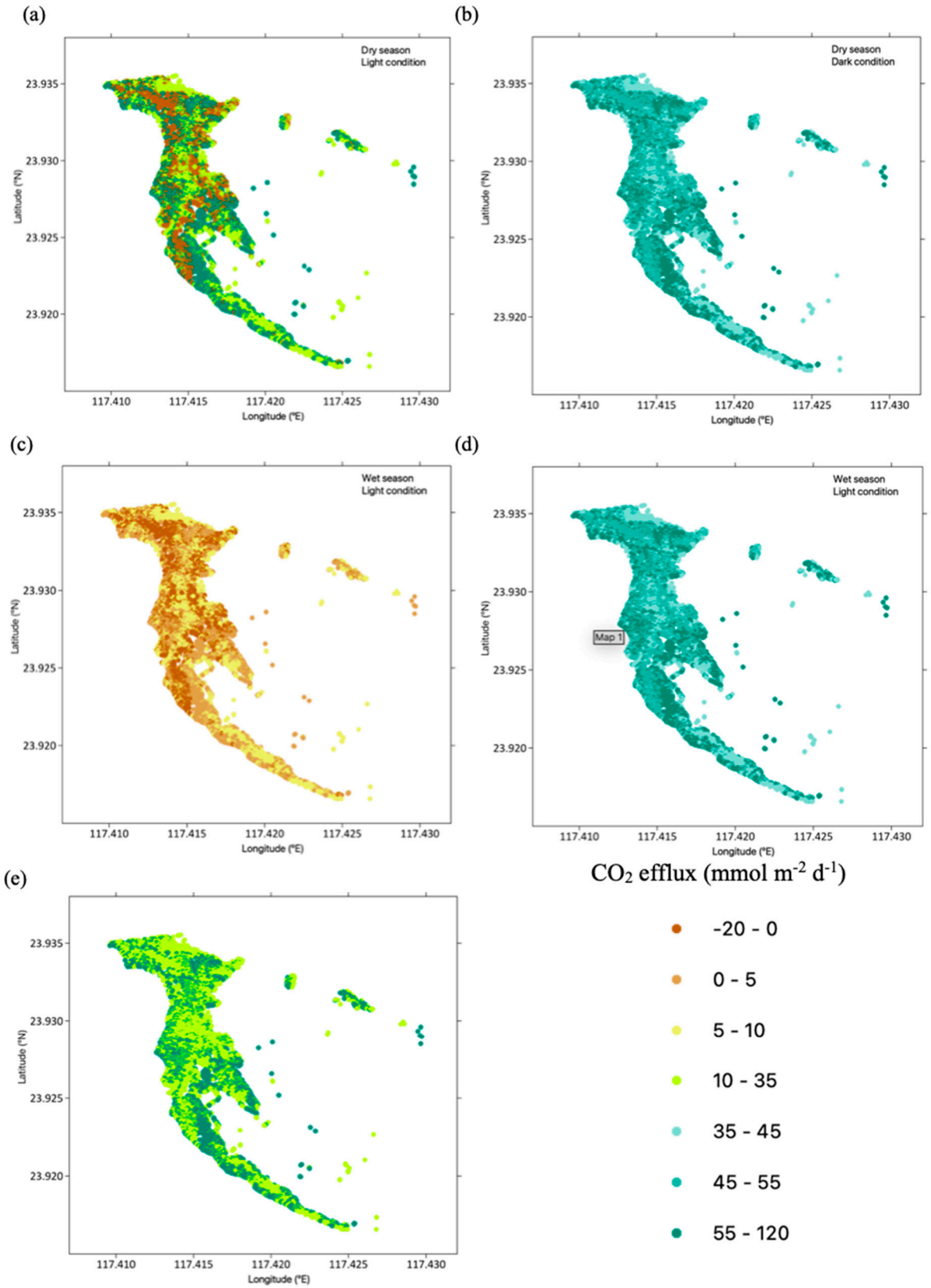

Figure 5. Spatial distribution of CO_2 efflux in Zhangjiangkou National Mangrove Nature Reserve. The panels show CO_2 efflux for dry seasons and light (**a**), dry seasons and dark (**b**), wet seasons and light (**c**), wet seasons and dark (**d**), and the average value combining seasons and light conditions (**e**).

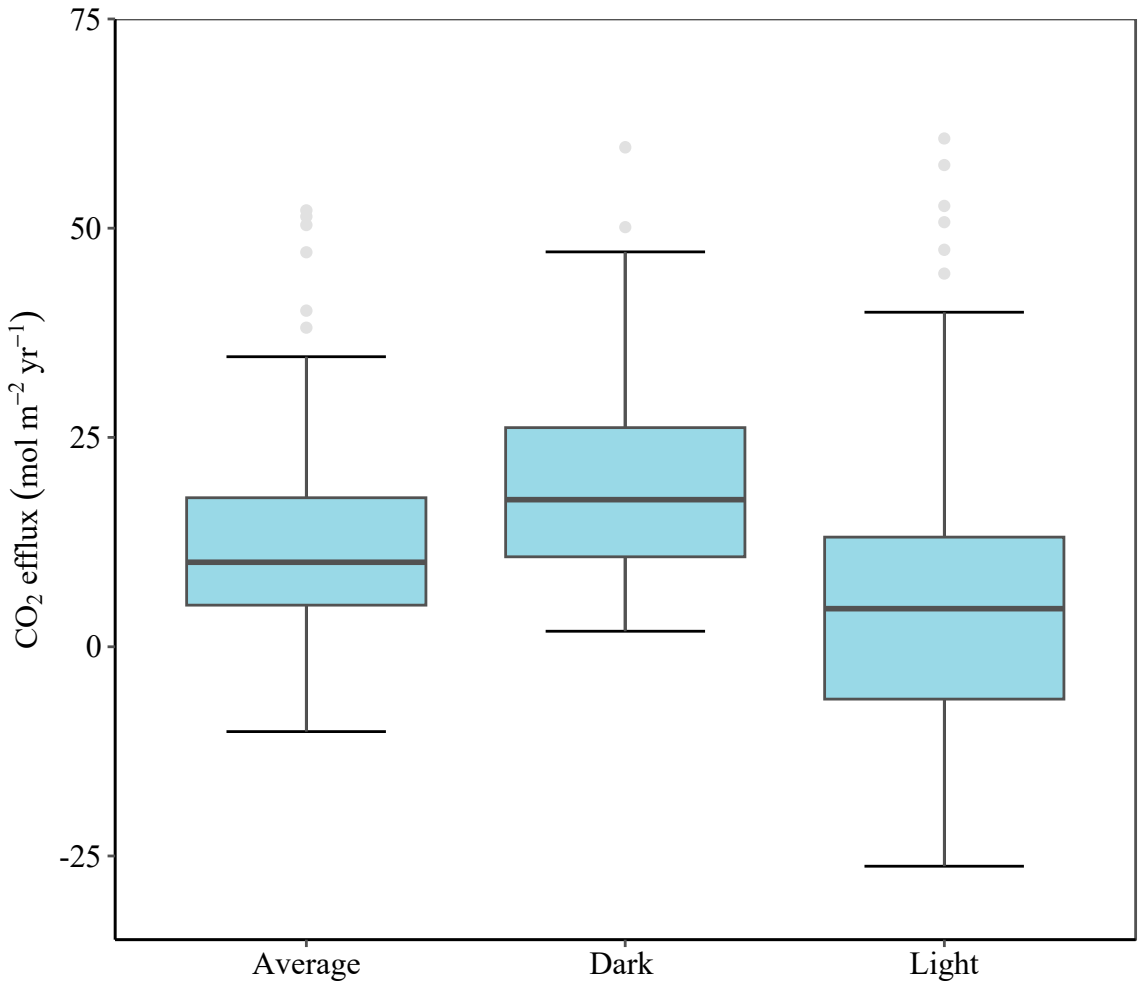

Figure 6. Annual CO_2 flux from the studied site. The grey points over the whiskers are outliers. The lower and upper hinges correspond to the 25th and 75th percentiles, respectively.

4. Discussion

4.1. Spatial and Seasonal Variation in CO_2 Flux

There is spatial and seasonal variation in CO_2 flux in the sampling site. CO_2 flux at the landward and middle sites was found to be significantly higher than that at the seaward sites, and was higher in the dry season (November) than that in the wet season (April) in 2015. The spatial variation in CO_2 flux is generally in line with the study by [17], in which contended CO_2 flux drops along the tidal gradient from landward to seaward. Further, landward positions at the studied area are subject to nutrient enrichment from aquaculture wastewater discharge, which may stimulate CO_2 flux [31]. The difference mainly reflects the fact that CO_2 is constrained by the water-logging conditions of the sediment, as is the seasonal difference, since microbial respiration may be hindered under high water levels [32]. Nonetheless, the average CO_2 flux from the landward sites is higher than that from the middle sites, but is not statistically different. The lack of a clear-cut pattern between the landward and middle sites may be due to confounding factors, such as stand stature, which determines substrate supply for microbial respiration. Mangrove tree heights are lower at the landward sites than those at the middle sites, especially *Aegiceras corniculatum* (landward sites ~1 m versus middle sites 3~4 m). Specifically, sulphate reduction tends to be the main anoxic pathway for sediment CO_2 production in mangroves. High stand stature from the same species may exudate more organic matter from live/dead root material [33], which was consumed by sulphate reducers to produce more CO_2. The average annual CO_2

flux at the studied site (13.6 ± 1.5 mol m^{-2} $year^{-1}$) is lower than the global average value of 56.5 ± 8.9 mmol m^{-2} day^{1} (i.e., 20.6 ± 3.2 mol m^{-2} $year^{-1}$) [34].

4.2. Biotic Controls on the Release of CO_2

Our result suggests that CO_2 flux varies with mangrove species and the number of biogenic structures (crab burrows and pneumatophores). The variation in CO_2 flux with mangrove species could also be primarily attributed to the density of pneumatophores, because pneumatophores are the major physiological characteristic of *Avicennia marina*, and are densely distributed in the mangroves. The impact of crab burrows on CO_2 release is dual; one is the heterotrophic respiration of crabs, and the other is the increase of CO_2 flux from burrows. Earlier investigation showed that the density of crab burrows was significantly higher in mangroves dominated by *Avicennia marina* than that of other mangroves in the studied site [35]. This result may also contribute to the higher sediment CO_2 flux of *Avicennia marina* relative to those of *Aegiceras corniculatum* and *Kandelia obovata*.

The increase of CO_2 by the biogenic structures of mangroves has been reported to be a more important portion of soil respiration in comparison with heterotrophic respiration. Mangrove sediments are featured with abundant biogenic structures. These structures alter the biogeochemical trade-off and enhance the exchange of solutes and gases several folds, making them important conduits that affect C dynamics in mangroves [36,37]. The enhancement of CO_2 release by pneumatophores is owing to the aerenchyma tissues.

Mangrove pneumatophores have open lenticels when exposed to air, not only permitting rapid diffusion of gases into (e.g., O_2) and from (e.g., CO_2) deep sediments through the air-filled aerenchyma tissue to the atmosphere [38,39], but also by stimulating sulphate reduction via root exudates [40,41]. In particular, the study shows that CO_2 flux increases linearly with pneumatophore densities, coinciding with the positive linear relationship between methane flux and pneumatophore densities [42].

Epibenthic burrows facilitate the exchange of nutrients and gases via increasing the area of sediment and air/water interfaces [43], as well as the transport of labile detritus to the subsurface layer during bioturbation activities [19]. In addition, crab burrows were suggested to considerably influence aeration, drainage, sediment chemistry and other conditions in our studied site [35].

From the regression analysis, the estimated CO_2 emission promoted by pneumatophores was 0.13 and 0.467 mmol $pneumatophore^{-1}$ d^{-1} for all and dark flux measurements, respectively. The increase of dark CO_2 flux due to pneumatophores is well within the range of reported values for dark flux, i.e., 0.26–0.66 mmol $pneumatophore^{-1}$ d^{-1} [19,37,44]. Likewise, the estimated CO_2 emission per burrow was 0.394 mmol $burrow^{-1}$ d^{-1} for all measurements. There may be at least one crab in each burrow (based on personal communication with local fishermen). Thus, this value also falls in the range of reported values (0.207–0.55 mmol $burrow^{-1}$ d^{-1}) for fiddle, ocypodid and grapsid crabs [19,44] when aggregating the increase of CO_2 emission by one crab and burrow. In particular, the estimated increase of CO_2 flux by burrows approaches the flux (0.39 mmol $burrow^{-1}$ d^{-1}) from [44] under sewage treatment, which is ~5× the flux without sewage treatment. Our studied mangrove site receives wastewater from adjacent aquaculture ponds. In addition, the disposal of wastewater in mangrove sediments initially leads to the enrichment of labile organic matter and nitrogen compounds. These nitrogen compounds are converted into nitrates and ammonium, which accelerate organic matter decomposition [45]. The high nutrient-enriched sewage from the ponds may promote sediment greenhouse gas emissions in mangroves [46], especially emissions from microbes inhabiting the burrow walls.

The data can be propagated from the individual biogenic structure to the unit area by averaging the number of biogenic structures under each chamber (0.099 m^2). Accordingly, the estimated CO_2 emission enhanced by biogenic structures was 18.29 mmol m^{-2} d^{-1} for pneumatophores and 15.52 mmol m^{-2} d^{-1} for crab burrows, which are the same order of magnitude reported in a mangrove forest in south-eastern Queensland, Australia by [47]. This could partly account for the significantly higher CO_2 flux of *Avicennia marina*

in relation to the other species, since pneumatophore densities are more than doubled in *Avicennia marina* compared with the overall mean. On the other hand, *Avicennia* generates oxic layers due to their allocation of O_2 to roots, and their root system is permeable [16]. The oxic conditions may facilitate OC decomposition and hence CO_2 production. Further, if excluding the influence of crab burrows and pneumatophores, CO_2 flux reaches 12.93 mmol m^{-2} d^{-1}, which falls in the global CO_2 flux from sediment surface in mangroves estimated by [5].

4.3. The Influence of Sediment Temperature and Light Conditions on CO_2 Flux

Sediment temperature is demonstrated to have a negative impact on CO_2 release. Moreover, when explored separately, sediment temperature has more of a negative impact on light CO_2 flux. Sediment temperature can be considered as a surrogate for light intensity during our sampling campaign. Higher sediment temperature designates more intensive sunlight, which promotes the photosynthetic activities of microphytobenthos (MPB) [18] and thereby assimilating more CO_2. In addition, by measuring the $\delta^{13}C$-CO_2 values of the CO_2 emitted under dark and light conditions, we were also able to confirm the reduction of CO_2 and its consumption during photosynthesis at the sediment surface [48]. This is also corroborated by the significantly higher dark flux relative to light flux in our study. Under dark conditions, the photosynthetic activity of MPB is limited while it is activated, and MPB uptakes CO_2 from the chamber under light conditions. Our inference is also underpinned by [49], which suggested that temperature and chlorophyll concentrations (a proxy for MPB abundance) were the main factors accounting for the variability of sediment CO_2 flux in a New Zealand mangrove.

Sediment temperature is one of the most influential factors regulating sediment greenhouse gas emissions [17], and high sediment temperature generally stimulates microbial respiration. However, sediment temperature was not found to have a relationship with dark flux; high sediment temperature in general corresponds to high air temperature which is negatively linked to CO_2 flux, as present in the formula of CO_2 flux calculation. Under light conditions, the negative impact of sediment temperature on CO_2 flux likely suggests that the MPB photosynthesis outreaches the impact of air temperature and microbial respiration. The extrapolation of variance explained by individual factors suggests that light is the most important factor driving the variation in CO_2 flux.

5. Conclusions

Our study shows that there is a significant relationship between sediment CO_2 flux and sediment temperature, the densities of crab burrows and pneumatophores, seasons, tidal positions and light conditions in a natural mangrove in Southern China, among which light conditions are the most important. Sediment CO_2 flux is controlled by a combination of spatial, temporal, biotic and physical factors. Further, sediment CO_2 flux at the landward and middle sites was significantly higher than that at seaward sites. CO_2 released from *Avicennia marina* was significantly faster than that from *Aegiceras corniculatum* and *Kandelia obovata*. CO_2 flux measured under dark conditions and dry seasons was higher than that measured under light conditions and wet seasons. Additionally, under the scenarios of two combined factors, CO_2 flux was significantly higher in *Avicennia marina* at landward and middle locations under dark conditions in dry seasons, and at middle locations under dark conditions, compared with others.

In particular, pneumatophores and crab burrows promote CO_2 release in the mangrove forest at a rate of 18.29 and 15.52 mmol m^{-2} d^{-1}, respectively. The increase of CO_2 flux by pneumatophores is mainly attributed to aerenchyma tissues, promoting CO_2 diffusion, but heterotrophic respiration (e.g., sulphate reduction) via root exudates is non-negligible. However, our study could not partition the two components, but the method of [50] provides the potential to address the issue. Future studies on NEP are expected to differentiate pneumatophore respiration and indirect heterotrophic respiration. The increase of CO_2 flux by burrows consists of crab respiration and the enhancement of CO_2 flux by burrows.

Further exploration of CO_2 flux from burrows of different crab species and sizes may provide clearer clues on the contribution of burrows to CO_2 flux.

Author Contributions: S.N., X.O., W.W., Z.Z., F.G., Z.Y. and S.Y.L. contributed to the conception and design of the study. S.N. and X.O. analyzed the data and wrote the initial version of the ms. W.W. and S.Y.L. critically revised the ms. All authors have read and agreed to the published version of the manuscript.

Funding: This study was supported by the National Natural Science Foundation of China (Nos. 52239005, 52271280), the Science and Technology Project of Guangdong Province (2022A0505050075), and the PI project of Southern Marine Science and Engineering Guangdong Laboratory (Guangzhou) (GML2022009).

Data Availability Statement: Data are available upon request sent to Xiaoguang Ouyang.

Acknowledgments: We cordially thank Qiucheng Wu who helped to coordinate the field work. We thank Xudong Zhu at Xiamen University for providing the map of species distribution and canopy height for the mangroves in the study site. Kaizhu Wu is appreciated for his assistance in the field.

Conflicts of Interest: There are no conflict of interest in this study.

References

1. Breithaupt, J.L.; Steinmuller, H.E. Refining the Global Estimate of Mangrove Carbon Burial Rates Using Sedimentary and Geomorphic Settings. *Geophys. Res. Lett.* **2022**, *49*, e2022GL100177. [CrossRef]
2. Donato, D.C.; Kauffman, J.B.; Murdiyarso, D.; Kurnianto, S.; Stidham, M.; Kanninen, M. Mangroves among the most carbon-rich forests in the tropics. *Nat. Geosci.* **2011**, *4*, 293–297. [CrossRef]
3. Alongi, D.M. Carbon Cycling and Storage in Mangrove Forests. *Annu. Rev. Mar. Sci.* **2014**, *6*, 195–219. [CrossRef] [PubMed]
4. McLeod, E.; Chmura, G.L.; Bouillon, S.; Salm, R.; Björk, M.; Duarte, C.M.; Lovelock, C.E.; Schlesinger, W.H.; Silliman, B.R. A blueprint for blue carbon: Toward an improved understanding of the role of vegetated coastal habitats in sequestering CO_2. *Front. Ecol. Environ.* **2011**, *9*, 552–560. [CrossRef]
5. Siikamäki, J.; Sanchirico, J.N.; Jardine, S.L. Global economic potential for reducing carbon dioxide emissions from mangrove loss. *Proc. Natl. Acad. Sci. USA* **2012**, *109*, 14369–14374. [CrossRef]
6. Doughty, C.L.; Langley, J.A.; Walker, W.S.; Feller, I.; Schaub, R.; Chapman, S.K. Mangrove Range Expansion Rapidly Increases Coastal Wetland Carbon Storage. *Estuaries Coasts* **2015**, *39*, 385–396. [CrossRef]
7. Richards, D.R.; Thompson, B.S.; Wijedasa, L. Quantifying net loss of global mangrove carbon stocks from 20 years of land cover change. *Nat. Commun.* **2020**, *11*, 426. [CrossRef]
8. Lee, S.Y.; Primavera, J.H.; Dahdouh-Guebas, F.; McKee, K.; Bosire, J.O.; Cannicci, S.; Diele, K.; Fromard, F.; Koedam, N.; Marchand, C.; et al. Ecological role and services of tropical mangrove ecosystems: A reassessment. *Glob. Ecol. Biogeogr.* **2014**, *23*, 726–743. [CrossRef]
9. Chambers, L.G.; Davis, S.E.; Troxler, T.; Boyer, J.N.; Downey-Wall, A.; Scinto, L.J. Biogeochemical effects of simulated sea level rise on carbon loss in an Everglades mangrove peat soil. *Hydrobiologia* **2013**, *726*, 195–211. [CrossRef]
10. Kirui, B.; Huxham, M.; Kairo, J.G.; Mencuccini, M.; Skov, M.W. Seasonal dynamics of soil carbon dioxide flux in a restored young mangrove plantation at Gazi Bay. In *Advances in Coastal Ecology: People, Processes and Ecosystems in Kenya*; Hoorweg, J.M.N., Ed.; African Studies Centre: Leiden, The Netherlands, 2009; Volume 20, pp. 122–130.
11. Ryan, M.G.; Law, B. Interpreting, measuring, and modeling soil respiration. *Biogeochemistry* **2005**, *73*, 3–27. [CrossRef]
12. Ouyang, X.; Kristensen, E.; Zimmer, M.; Thornber, C.; Yang, Z.; Lee, S.Y. Response of macrophyte litter decomposition in global blue carbon ecosystems to climate change. *Glob. Chang. Biol.* **2023**. [CrossRef]
13. Hanson, P.J.; Edwards, N.T.; Garten, C.T.; Andrews, J.A. Separating root and soil microbial contributions to soil respiration: A review of methods and observations. *Biogeochemistry* **2000**, *48*, 115–146. [CrossRef]
14. Lee, M.-S.; Nakane, K.; Nakatsubo, T.; Koizumi, H. Seasonal changes in the contribution of root respiration to total soil respiration in a cool-temperate deciduous forest. *Plant Soil* **2003**, *255*, 311–318. [CrossRef]
15. Bouillon, S.; Borges, A.V.; Castaneda, E.; Diele, K.; Dittmar, T.; Duke, N.C.; Kristensen, E.; Lee, S.Y.; Marchand, C.; Middelburg, J.; et al. Mangrove production and carbon sinks: A revision of global budget estimates. *Glob. Biogeochem. Cycles* **2008**, *22*. [CrossRef]
16. Alongi, D.M. *The Energetics of Mangrove Forests*; Springer: New York, NY, USA, 2009; p. 216.
17. Chen, G.C.; Tam, N.F.; Ye, Y. Spatial and seasonal variations of atmospheric N2O and CO2 fluxes from a subtropical mangrove swamp and their relationships with soil characteristics. *Soil Biol. Biochem.* **2012**, *48*, 175–181. [CrossRef]
18. Leopold, A.; Marchand, C.; Deborde, J.; Chaduteau, C.; Allenbach, M. Influence of mangrove zonation on CO_2 fluxes at the sediment–air interface (New Caledonia). *Geoderma* **2013**, *202–203*, 62–70. [CrossRef]
19. Kristensen, E.; Flindt, M.; Ulomi, S.; Borges, A.; Abril, G.; Bouillon, S. Emission of CO2 and CH4 to the atmosphere by sediments and open waters in two Tanzanian mangrove forests. *Mar. Ecol. Prog. Ser.* **2008**, *370*, 53–67. [CrossRef]

20. Sheng, N.; Wu, F.; Liao, B.; Xin, K. Methane and carbon dioxide emissions from cultivated and native mangrove species in Dongzhai Harbor, Hainan. *Ecol. Eng.* **2021**, *168*, 106285. [CrossRef]
21. Liu, M.; Mao, D.; Wang, Z.; Li, L.; Man, W.; Jia, M.; Ren, C.; Zhang, Y. Rapid Invasion of Spartina alterniflora in the Coastal Zone of Mainland China: New Observations from Landsat OLI Images. *Remote Sens.* **2018**, *10*, 1933. [CrossRef]
22. Zhang, Y.; Huang, G.; Wang, W.; Chen, L.; Lin, G. Interactions between mangroves and exotic Spartina in an anthropogenically disturbed estuary in southern China. *Ecology* **2012**, *93*, 588–597. [CrossRef]
23. Xu, L.; Furtaw, M.D.; Madsen, R.A.; Garcia, R.L.; Anderson, D.J.; McDermitt, D.K. On maintaining pressure equilibrium between a soil CO_2 flux chamber and the ambient air. *J. Geophys. Res. Atmos.* **2006**, *111*, D08. [CrossRef]
24. Jensen, L.; Mueller, T.; Tate, K.; Ross, D.; Magid, J.; Nielsen, N. Soil surface CO2 flux as an index of soil respiration in situ: A comparison of two chamber methods. *Soil Biol. Biochem.* **1996**, *28*, 1297–1306. [CrossRef]
25. Kabwe, L.; Hendry, M.; Wilson, G.; Lawrence, J. Quantifying CO2 fluxes from soil surfaces to the atmosphere. *J. Hydrol.* **2002**, *260*, 1–14. [CrossRef]
26. Zhu, X.; Hou, Y.; Weng, Q.; Chen, L. Integrating UAV optical imagery and LiDAR data for assessing the spatial relationship between mangrove and inundation across a subtropical estuarine wetland. *ISPRS J. Photogramm. Remote Sens.* **2019**, *149*, 146–156. [CrossRef]
27. R Core Team. *A Language and Environment for Statistical Computing*; R Foundation for Statistical Computing: Vienna, Austria, 2023.
28. Aho, K. *asbio: A Collection of Statistical Tools for Biologists*, R package version 1.2-5; CRC/Taylor and Francis: Boca Raton, FL, USA, 2015.
29. Fox, J.; Weisberg, S. *An [1] Companion to Applied Regression*, 2nd ed.; Sage: Thousand Oaks, CA, USA, 2011.
30. Grömping, U. Relative importance for linear regression in R: The package relaimpo. *J. Stat. Softw.* **2006**, *17*, 1–27. [CrossRef]
31. Barroso, G.C.; Abril, G.; Machado, W.; Abuchacra, R.C.; Peixoto, R.B.; Bernardes, M.; Marques, G.S.; Sanders, C.J.; Oliveira, G.B.; Filho, S.R.O.; et al. Linking eutrophication to carbon dioxide and methane emissions from exposed mangrove soils along an urban gradient. *Sci. Total. Environ.* **2022**, *850*, 157988. [CrossRef] [PubMed]
32. Poungparn, S.; Komiyama, A.; Tanaka, A.; Sangtiean, T.; Maknual, C.; Kato, S.; Tanapermpool, P.; Patanaponpaiboon, P. Carbon dioxide emission through soil respiration in a secondary mangrove forest of eastern Thailand. *J. Trop. Ecol.* **2009**, *25*, 393–400. [CrossRef]
33. Dittmar, T.; Lara, R.J. Molecular evidence for lignin degradation in sulfate reducing mangrove sediments (Amazonia, Brazil). *Geochim. Cosmochim. Acta* **2001**, *65*, 1403–1414. [CrossRef]
34. Rosentreter, J.A.; Maher, D.; Erler, D.; Murray, R.; Eyre, B. Seasonal and temporal CO2 dynamics in three tropical mangrove creeks—A revision of global mangrove CO2 emissions. *Geochim. et Cosmochim. Acta* **2018**, *222*, 729–745. [CrossRef]
35. Wang, M.; Gao, X.; Wang, W. Differences in burrow morphology of crabs between Spartina alterniflora marsh and mangrove habitats. *Ecol. Eng.* **2014**, *69*, 213–219. [CrossRef]
36. Holmer, M.; Andersen, F.; Holmboe, N.; Kristensen, E.; Thongtham, N. Transformation and exchange processes in the Bangrong mangrove forest-seagrass bed system, Thailand. Seasonal and spatial variations in benthic metabolism and sulfur biogeochemistry. *Aquat. Microb. Ecol.* **1999**, *20*, 203–212. [CrossRef]
37. Kitaya, Y.; Yabuki, K.; Kiyota, M.; Tani, A.; Hirano, T.; Aiga, I. Gas exchange and oxygen concentration in pneumatophores and prop roots of four mangrove species. *Trees* **2002**, *16*, 155–158. [CrossRef]
38. Purnobasuki, H.; Suzuki, M. Aerenchyma tissue development and gas-pathway structure in root of *Avicennia marina* (Forsk.) Vierh. *J. Plant Res.* **2005**, *118*, 285–294. [CrossRef]
39. Purnobasuki, H.; Suzuki, M. Aerenchyma formation and porosity in root of a mangrove plant, Sonneratia alba (*Lythraceae*). *J. Plant Res.* **2004**, *117*, 465–472. [CrossRef]
40. Alongi, D.; Sasekumar, A.; Tirendi, F.; Dixon, P. The influence of stand age on benthic decomposition and recycling of organic matter in managed mangrove forests of Malaysia. *J. Exp. Mar. Biol. Ecol.* **1998**, *225*, 197–218. [CrossRef]
41. Kristensen, E.; Alongi, D.M. Control by fiddler crabs (Uca vocans) and plant roots (*Avicennia marina*) on carbon, iron, and sulfur biogeochemistry in mangrove sediment. *Limnol. Oceanogr.* **2006**, *51*, 1557–1571. [CrossRef]
42. Livesley, S.J.; Andrusiak, S.M. Temperate mangrove and salt marsh sediments are a small methane and nitrous oxide source but important carbon store. *Estuarine, Coast. Shelf Sci.* **2012**, *97*, 19–27. [CrossRef]
43. Lee, S. Mangrove macrobenthos: Assemblages, services, and linkages. *J. Sea Res.* **2008**, *59*, 16–29. [CrossRef]
44. Penha-Lopes, G.; Kristensen, E.; Flindt, M.; Mangion, P.; Bouillon, S.; Paula, J. The role of biogenic structures on the biogeochemical functioning of mangrove constructed wetlands sediments—A mesocosm approach. *Mar. Pollut. Bull.* **2010**, *60*, 560–572. [CrossRef]
45. Queiroz, H.M.; Artur, A.G.; Taniguchi, C.A.K.; da Silveira, M.R.S.; Nascimento, J.C.D.; Nóbrega, G.N.; Otero, X.L.; Ferreira, T.O. Hidden contribution of shrimp farming effluents to greenhouse gas emissions from mangrove soils. *Estuarine Coast. Shelf Sci.* **2019**, *221*, 8–14. [CrossRef]
46. Ouyang, X.; Guo, F. Paradigms of mangroves in treatment of anthropogenic wastewater pollution. *Sci. Total. Environ.* **2016**, *544*, 971–979. [CrossRef] [PubMed]
47. Ouyang, X.; Lee, S.Y.; Connolly, R.M. Structural equation modelling reveals factors regulating surface sediment organic carbon content and CO2 efflux in a subtropical mangrove. *Sci. Total. Environ.* **2017**, *578*, 513–522. [CrossRef] [PubMed]
48. Jacotot, A.; Marchand, C.; Allenbach, M. Biofilm and temperature controls on greenhouse gas (CO2 and CH4) emissions from a Rhizophora mangrove soil (New Caledonia). *Sci. Total. Environ.* **2019**, *650*, 1019–1028. [CrossRef] [PubMed]

49. Bulmer, R.H.; Lundquist, C.J.; Schwendenmann, L. Sediment properties and CO2 efflux from intact and cleared temperate mangrove forests. *Biogeosciences* **2015**, *12*, 6169–6180. [CrossRef]
50. Ouyang, X.; Lee, S.Y.; Connolly, R.M. Using isotope labeling to partition sources of CO_2 efflux in newly established mangrove seedlings. *Limnol. Oceanogr.* **2017**, *63*, 731–740. [CrossRef]